

Mechanical Property Optimization of FDM PLA in Shear with Multiple Objectives

JONATHAN TORRES,^{1,2} JOSÉ COTELO,¹ JUSTIN KARL,¹ and ALI P. GORDON¹

1.—Department of Mechanical and Aerospace Engineering, University of Central Florida, Orlando, FL 32816, USA. 2.—e-mail: jonathantorres@knights.ucf.edu

This study presents the influences of key processing parameters on the resulting material properties of fused-deposition-modeled (FDM) polylactic acid (PLA) components tested in torsion. A reduced experimental matrix was produced through the use of a Taguchi L9 orthogonal array with three parameters at three levels each. The processing parameters included the layer thickness, infill density, and postprocessing heat-treatment time at 100°C. Testing of components at varying times is conducted to facilitate heat-treatment time testing range and show the effects of prolonged heating. The layer thickness and infill are tested across the entire useful range available for the FDM machine used. Shear stress–strain response curves are acquired and average ultimate shear strength, 0.2% yield strength, proportional limit, shear modulus, and fracture strain are calculated for each run. An analysis of results via regression analysis is used to determine influences levels of parameters of the mechanical properties. The layer thickness and infill density are shown to be of high importance when optimizing for strength, with heat-treatment implementation slightly improving the resulting properties. Ductility is mainly affected by infill and heat treatment, with layer thickness having only a slight effect on the fracture strain achieved. Recommendations are made based on results of a method to optimize for either strength or ductility and how to compromise between recommended settings when a balance between the two is desired. The ability to produce parts with mechanical properties at or near those of bulk PLA is shown.

INTRODUCTION

Proliferation of rapid prototyping (RP) and rapid manufacturing technologies has steadily progressed in the past three decades, moving from the first commercially-available stereolithography (SLA) hardware in the late 1980s to the desktop-sized fused-deposition modeling (FDM) systems of today. The aforementioned types of systems along with several others are all variances on the concept of additive manufacturing. In this family of methods, three-dimensional objects are created by building layer upon layer via material delivery along two-dimensional tool paths.

Most recently, a number of factors have led to exponential growth in the use of such systems, with the largest gains coming from the lower-cost thermoplastic extrusion FDM consumer market. An

expiration of key patents in 2009 and economies of scale in component supply chains have driven widescale adoption by hobbyists, students, and research and development laboratories in both academia and commercial settings.

With high levels of utilization in a number of industries, need arises for proper mechanical evaluation of the resulting printed parts. The most common source materials for commercially-available FDM printers are acrylonitrile butadiene styrene (ABS) and polylactic acid (PLA). While each of these thermoplastics has well-characterized behavior, the ultimate behavior of a macro-scale printed component is highly dependent on the complex patterned layer structure established during the printing process. The characteristics of bulk PLA^{1–3} are available in Table I.

Table I. Material properties of bulk polylactic acid as found via literature review¹⁻³

Material property	Units	Value
Density (ρ)	g/cm ³	1.24
Elastic modulus (E)	MPa	3500
Shear modulus (G)	MPa	1287
Poisson's ratio (ν)	–	0.36
Yield strength (σ_y)	MPa	70
Ultimate tensile strength (S_{ut})	MPa	73
Elongation	%	~7

An examination of the dependencies on controllable printer parameters can lead to optimized components from each of the source materials. Print orientation and infill density alone have been shown to alter compressive, tensile, flexural, and impact strengths by an order of magnitude in some cases.⁴⁻⁶ While significant work of this nature has been performed with ABS, only recently has PLA been the subject of such a study. Industrial and general use of PLA is increasingly more popular due to its environmental friendliness and biocompatibility, and many desktop consumer printer models now exclusively use PLA. As a consequence, scrutiny now falls on the user-controllable aspects of the FDM process and the resultant effect on PLA parts.

Although some mechanical properties of PLA have been studied more thoroughly, there is little to no information on property evaluation under shear loading. Therefore, a direct aim of this specific research is to provide characterization and printer parameter optimization information for PLA parts intended to primarily be subjected to torsion loads. Additionally, the effect of a postmanufacturing temperature treatment is considered. After printing, PLA can be annealed to promote microstructural changes that improve uniformity, relieve stresses, and strengthen the PLA part. By extending the time at elevated temperatures below the glass transition point, PLA has been shown to increase crystallinity, which leads to superior tensile and flexural strength and stiffness.^{7,8} Consequently, it may be inferred that the effects of both annealing temperature and time will have noteworthy effects on resulting shear properties.

A similar study was previously carried out in Part I⁹ to characterize and optimize the PLA parts loaded in the tensile sense. As shown by the results of the previous study, a significant number of parameters can be evaluated without the need for a full factorial experiment (FFE) program. A reduced number of specimens can be tested in conjunction with the application of the Taguchi design of experiments (DoE) method and analysis of variance (ANOVA). The use of a Taguchi matrix can minimize the number of experiments necessary while creating a correlation between process parameters to optimize select material properties and attempt to compro-

mise between properties which can require conflicting process settings to suggest an overall optimized solution to promote all properties. In the case of this work, DoE was applied to determine an experimental matrix of factors that include printer settings and postprocessing levels. Analysis of results via the ANOVA method is used to determine the factor impact on 0.2% yield strength, ultimate shear strength, proportional limit, fracture strain, and shear modulus.

EXPERIMENTAL

Background Topics and Method Justification

The motivation for this study is twofold. First, as additive manufacturing with PLA continues to mature and grow in popularity, increasing the knowledge base of these topics both independently and in tangent becomes ever more important. This research strives to aid in advancing both the manufacturing processes and the materials involved by providing data and methodologies for RP users and manufacturers with specific objectives. Second, this effort reinforces and expands the validity of the processes described in our previous study, which provided a method for the optimization of mechanical properties of FDM PLA in tension and fracture. An expanded experimental array with an increased factor level and more thorough analysis explores the effects of interactions between parameters on material properties and the possibility of using these methods for multiobjective optimization.

Few testing standards exist for additive manufactured components largely due to variability amongst methods and processes; most standards are based on terminology and reporting guidelines. The ASTM E143 torsion testing standard is the most relevant, although this standard is not nearly as rigorous in its requirements for samples and testing procedures than those for tensile and fracture. The relevant standards for fused deposition modeling include ASTM F2792 for general terminology, ASTM F2791 for data reporting purposes, and ISO/ASTM 52921 for generalized guidelines related to test methodologies and coordinate systems in component manufacturing. These ISO/ASTM guidelines were referenced for both testing and reporting during experimental methodology, data analysis, and report preparation. Heat deflection temperatures were measured as outlined in ASTM D648.

FDM Printer Setting Selection

The samples were manufactured in an XY orientation, with the X direction being the long direction parallel to the front of the build plate. The first sample for each subset of three was centered on the build plate with the other two samples manufactured for that run placed directly in front and be-

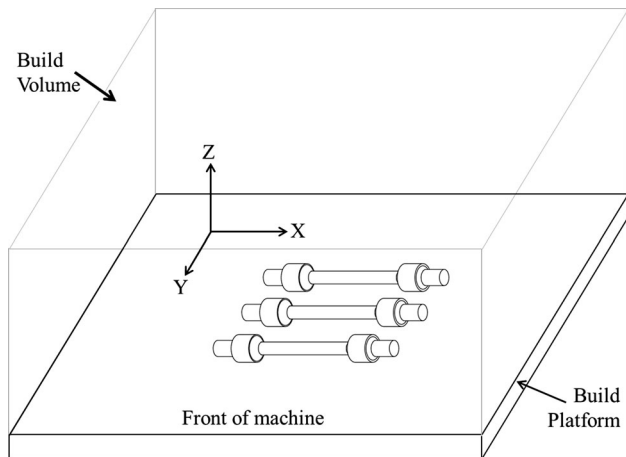


Fig. 1. Part location and orientation during build: three samples printed in the center of the build platform in the XY orientation.

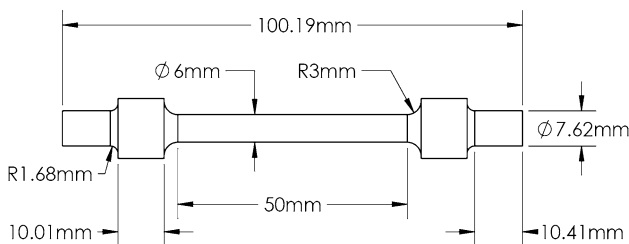


Fig. 2. Torsion specimen design and dimensions.

hind it with a minimal gap in between, as shown in Fig. 1. Due to the sample geometry, the need to test in the YX direction is nullified, as the samples would be identical in this orientation. Testing of samples manufactured in the ZX (or ZY) direction was forgone as preliminary tests indicated that torsion samples will delaminate before deforming when manufactured in this orientation. The samples were produced in a climate-controlled ambient environment, at 20°C and minimal humidity with a Makerbot Replicator 2 (MakerBot Industries LLC, Brooklyn, NY). The extruder temperature was set to 230°C, the number of perimeter layers set at 2, and the linear travel speed set to 90 mm/s for all samples. These are the manufacturer default levels for these settings, as well as the recommended settings for general use as shown in our previous paper. A schematic of the samples under examination can be seen in Fig. 2.

Numerous processing parameters can be explored in a study such as this, yet previous experimentation⁹ supports that only some key parameters warrant scrutiny when a new study is based on the same combination of production technology and material. The extruder nozzle temperature of 230°C corresponds to a material temperature of 180°C; this setting is optimized for the formation of components with the least warping and the highest

strength values. The speed setting of 90 mm/s had little effect on material properties in the previous study. The infill direction was shown to have little effect on the results, although additional complexity was introduced when producing parts. To alter the default infill pattern, an external slicing program and custom script must be used. A square-gridded pattern that can be angularly reoriented is helpful in drawing out directional dependencies. The hexagonal infill pattern, which is standard to many extrusion printers including the Replicator 2, does not lend itself to property reliance on infill orientation. Thus, this factor was also eliminated. Finally, the dependency contribution of the perimeter layer is well established, and the prior work showed the importance of component strength. Of the typically altered parameters, this leaves only the layer height and percentage infill to be explored, both of which have been shown to be of high importance.^{9,10} Additionally, heat treatment as a finishing step for components produced from PLA is a growing topic of discussion among desktop FDM users. Preliminary bench tests using a directed air heat source on samples for varying periods of time revealed significant differences in the tensile and torsional behaviors of otherwise identical components. Intrinsically, postmanufacturing heat treatment of FDM PLA components becomes as important as some fundamental printer settings. As such, the effect of altering the duration of such a process will be examined.

Heat Treatment of PLA

Previous literature emphasizes the influence of postprocess annealing on certain mechanical properties in tensile loading. In simplistic tests, increases in tensile modulus and heat deflection temperature (HDT) versus neat PLA are noted after annealing at 100°C.¹¹ At lower temperatures, tensile modulus also increases with both temperature and anneal times in the 65–80°C and 15–60 min range, respectively. From Ref. ¹², there is a clear indication that in temperature ranges from 65°C to 80°C rigidity, fracture toughness and HDT in PLA samples also increase proportionally with temperature. Toughness and rigidity acquired postanneal are attributed to a crystallinity increase with an associated increase in secondary bonds, thereby forming a less fluid material with increased stability and heat resistance at higher temperatures.¹³ An increase in useful ductility range coupled with an increase in crystallinity due to recrystallization effects is also correlated with the annealing process. Flexure-related properties are augmented by post-processing annealing, with trials between 30 and 60 min at annealing temperatures of 80°C, the flexural modulus, strength, and HDT increase in direct proportion to annealing time.¹⁴

Near or beyond 60 min, no further notable increase in strength or modulus occurs. After this

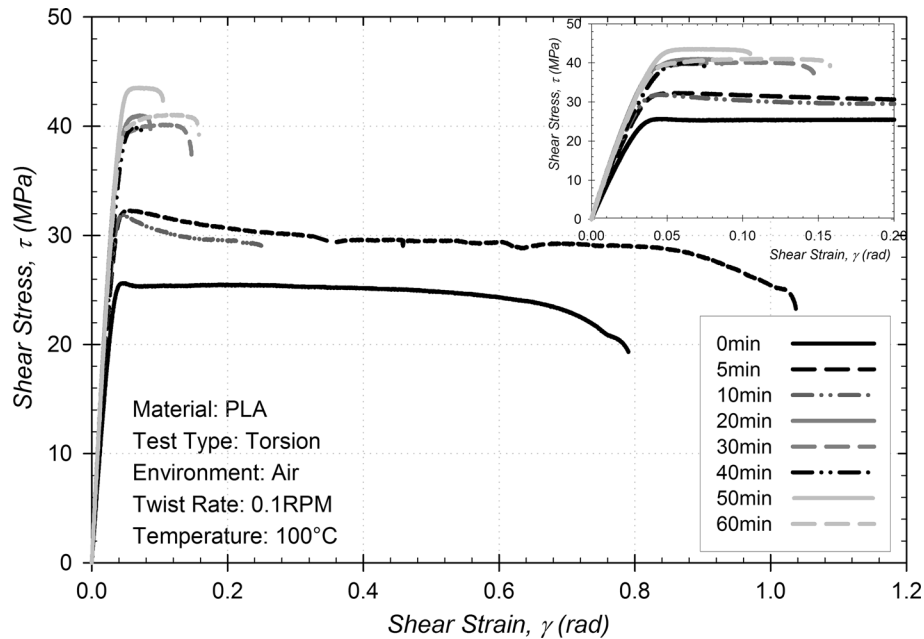


Fig. 3. Stress–strain response of 0.1-mm layer thickness, 20% infill components heated for various times of 0–60 min at 100°C.

point, there is no further increase in crystallinity, yielding a lack of improved mechanical properties. In several trials lasting longer than 1 h, the modulus and strength properties degraded to or fell below that of the neat PLA.¹⁵ This decrease may be tied to the material reorganizing weaker bonds internally after specific time intervals of thermal treatment allow for enough energy input.

Increases in tensile modulus have been reported at annealing temperatures of both 70°C and 100°C, although maximum modulus values remain in the domain of 100°C only.¹⁴ Additionally, Harris and Lee¹⁴ reported a decrease of fracture strain with increased annealing. Thus, a relationship between fracture strain and annealing time will also be explored to validate current findings in literature. Furthermore, it is suggested that a 100°C treatment of 10 min allows PLA to recrystallize with an optimal internal filament arrangement, a by-product of lower porosity due to induced thermal bonding.¹⁶ From these converging sources, a heat-treatment temperature of 100°C was chosen as optimal for further experimentation.

A preliminary experiment was carried out to determine the heat-treatment times of interest for the study. The torsion samples identical to those employed within the main test matrix of this study were manufactured with 0.1 mm layer thickness and 20% infill, as these components were theorized as being the most susceptible to any effects likely to be incurred from heat treatment. Along with a control sample that did not undergo any heat treatment, the parts were heated for 5 min, 10 min, 20 min, 30 min, 40 min, 50 min, and 60 min at 100°C, and then they were tested in torsion at a rate of 0.1 rpm. Strong time-dependent effects were

noted at annealing times up to 20 min, consequently creating an upper limit for annealing time for this study.

The stress–strain curves of the 5- and 10-min trials in Fig. 3 reveal an identical increase in ultimate shear stress, while the 5-min trial also indicates an increase in shear strain. This implies that a period of 10 min may be the start of the increased crystallization and subsequent brittle transition. Beyond 10 min, all of the following annealing times showed very high stress levels and very low strain levels in the specimens at failure, indicating brittle behavior. With increased scatter but no discernible trend beyond, the 20-min annealing length was chosen as the upper limit to be representative of this grouping of high heating times.

Experimental Parameters and Methodology

Based on findings from the previous study, preliminary heat-treatment testing, and literature reviews including manufacturer recommendations, the following conditions and related parameters were chosen for the study:

- Print layer thickness varied across the full available range of the printer, from 0.1-mm layers to 0.3-mm layers, in increments of 0.1 mm.
- Infill relative densities from 20% (lower limit of useful structural parts) to 100% (solid parts) in increments of 40%.
- Postprint heat treatments at 100°C with anneal times of 0 min, 5 min, and 20 min to coincide with zero, low, and high recrystallization levels.

These settings are summarized in Table II. With three process parameters each carrying three levels

Table II. Ranges of process parameters employed in this study and the corresponding low, middle, and high settings for each

Process parameter	Range	Low	Middle	High
Layer thickness (δ)	0.1–0.3 mm	0.1	0.2	0.3
Percent infill (ρ)	0–100%	20	60	100
Heat treatment (HT)	0–20 min	0	5	20

Table III. Run definition via implementation of an L9 Taguchi orthogonal array

L9 array	Process parameters		
	δ (mm)	P (%)	HT (min)
Run			
1	0.1	20	0
2	0.1	60	5
3	0.1	100	20
4	0.2	20	5
5	0.2	60	20
6	0.2	100	0
7	0.3	20	20
8	0.3	60	0
9	0.3	100	5

of interest, a Taguchi L9 orthogonal array was constructed to test the impact of layer thickness, infill, and heat treatment on a variety of material properties. Three identical repetitions for each experiment lead to a total of 27 experiments, which is reduced versus a full factorial set that would require $3^3 \times 3$, or 81, experiments. The Taguchi array designed for this experiment is shown in Table III.

Heat treatment of samples was conducted using a Barnstead Thermolyne F48055 (Hogentogler & Co. Inc., Columbia, MD) resistance furnace. The furnace was preheated to 100°C and heat soaked for 30 min prior to specimen insertion. A Eurotherm 2416 temperature controller (Schneider Electric, Ashburn, VA) provided furnace control and readout via feedback from a type K thermocouple. The specimens were treated in batches of three with their testing counterparts and removed promptly from the furnace at the end of the treatment. Cooling in the ambient air environment occurred before the length and diameters of the gage sections of each sample were measured and recorded.

After preparation, the samples were secured in the test device, an MTS Bionix Electromechanical Torsion tester (model no. 100-224-094; MTS Systems Corporation, Eden Prairie, MN) with a 50-Nm capacity. Chuck-style grips were hand tightened to avoid compressing sample ends while providing a grip in which no slippage could occur, shown in Fig. 4. The samples were fixed at one end and then torqued at the other at a slow rate of 0.1 rpm to insure that no strain-dependent effects were introduced. Data in the form of a torque-twist curve were obtained at a rate of 100 Hz.

MECHANICAL EXPERIMENTATION RESULTS

A mechanical response was characterized in the form of shear stress versus shear strain. Shear stress τ is defined as

$$\tau = \frac{TD}{2J} \quad (1)$$

where J , the polar moment of inertia, is calculated as

$$J = \frac{\pi D^4}{32} \quad (2)$$

and shear strain γ was defined as

$$\gamma = \frac{\theta D}{2L} \quad (3)$$

where T is the torque as measured by the torsion load cell, D is the diameter at the gage section, L is the gage length, and θ is the angular displacement. A typical response curve for each of the trials is shown in Fig. 5 for a direct comparison. Although some grouping is evident, it is apparent that the various combinations of processing properties associated with the different tests yield highly diverse responses.

To properly quantify these differences, the mechanical shear properties of the specimens were calculated and compared. The properties evaluated include strength indicators such as 0.2% offset shear yield strength τ_y and ultimate shear strength S_{us} . The proportional limit τ_{pl} is evaluated to signify the primary transition from elastic to plastic behavior, and shear modulus G quantifies the materials response to shear stress and is defined as ratio of shear stress to shear strain during elastic response. Ductility, the ability of the part to deform before failure, is quantified by the strain at fracture γ_f . The average values for each of these properties were calculated for each trial and quantified in Fig. 6. The graph containing G and γ_f uses a normalized average value for these properties, calculated by dividing the averages by the maximum sampled value, that is, the highest value found among the 27 samples tested. The maximum values found were 1312.5 MPa and 3.4454 mm/mm for the shear modulus and fracture strain, respectively.

The metrics that quantify strength all follow an identifiable pattern. Comparing the graphs of Fig. 6

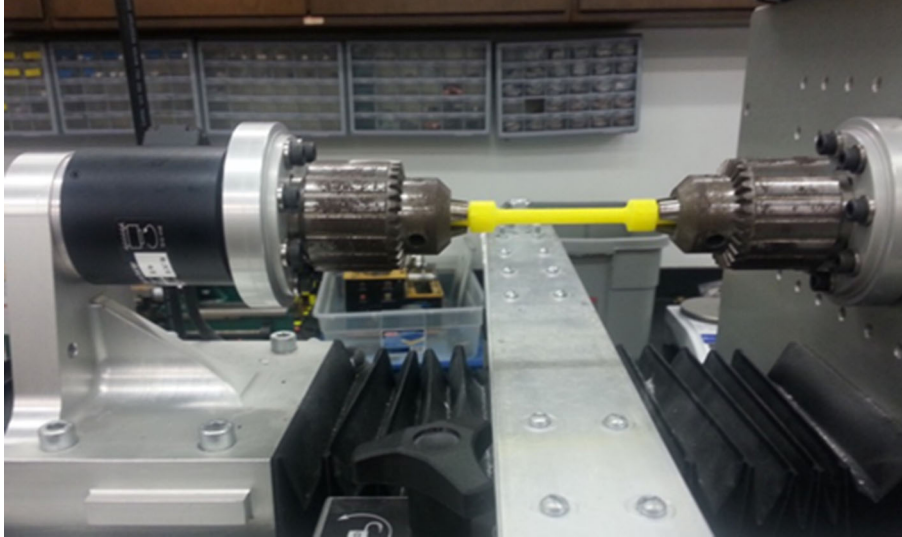


Fig. 4. Torsion specimen during testing in an MTS Bionix Electromechanical Torsion Tester.

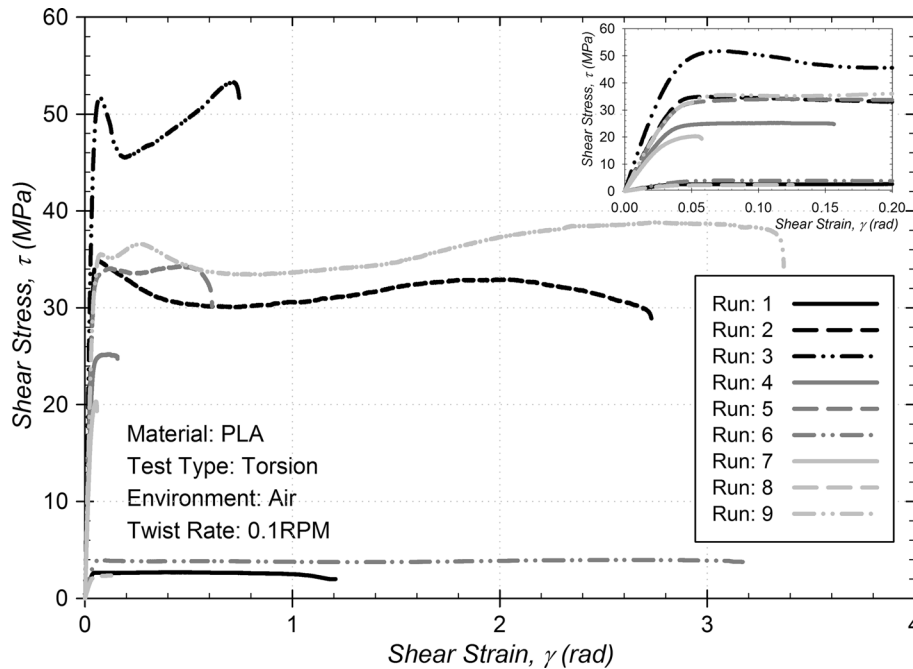


Fig. 5. Typical stress–strain response curves characteristic of each run.

versus the test matrix, it is noted that strength rises with increasing infill percentages. This finding is logical, as components with higher levels of infill physically contain more material to resist deformation. In a more localized view, a pattern is evident in trials 1–3, 4–6, and 7–9 in Fig. 6a. This correlates inversely with a change in layer thickness, as a decrease in strength is seen with increasing layer thickness. This is hypothesized to be related to thinner layers containing smaller gaps between the extruded strands and thus having overall lower porosity, or it could be that a greater number of

smaller strands clustered together results in higher resistance to deformation.

Torsional rigidity response in Fig. 6b has a similar pattern to the strength metrics, although the shear modulus is dependent on the parameter values to a lesser degree. The fracture strain does not follow a likewise trend. The three trials with the highest average fracture strain in descending order, runs 9, 6, and 2, also have high infill levels of 100%, 100%, and 60%, with seemingly little dependency on layer thickness. Trial 3, however, which also uses 100% infill and yields the highest strength values,

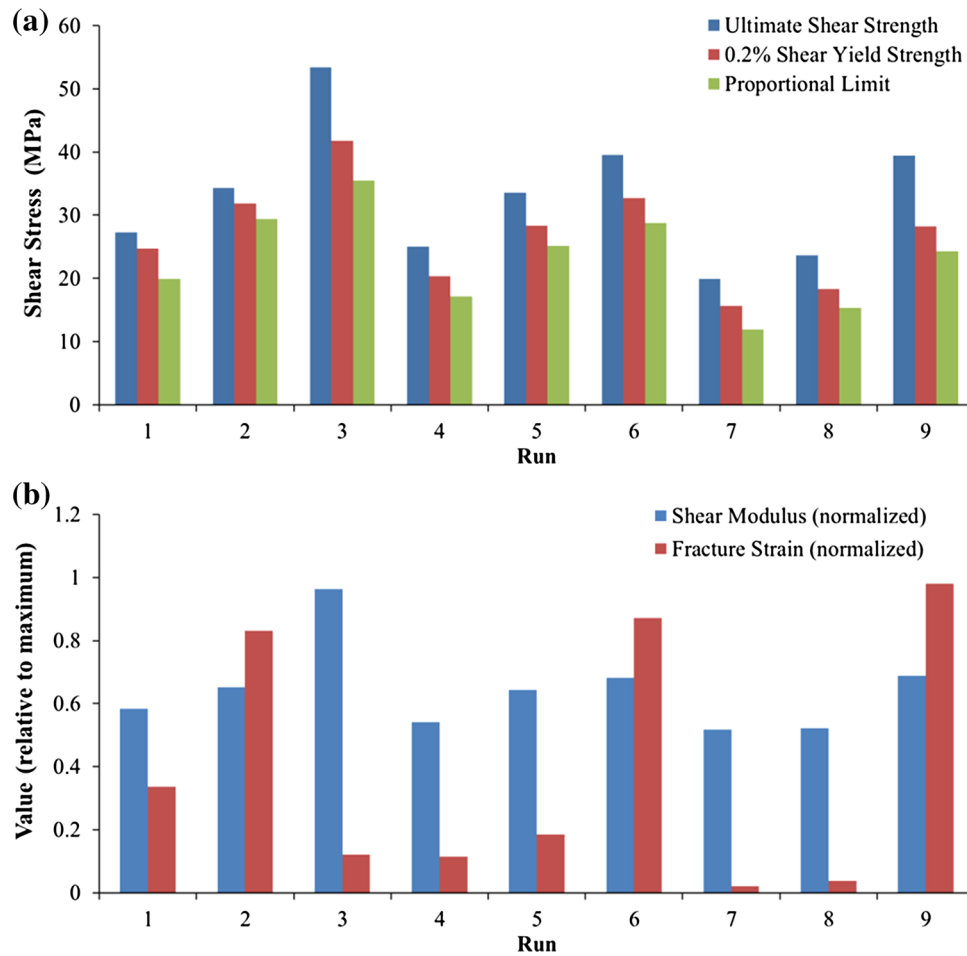


Fig. 6. Comparison of the average shear properties across all runs showing (a) ultimate shear strength S_{US} , 0.2% shear yield strength τ_y , proportional limit τ_{pl} , and (b) the normalized values of shear modulus G and fracture strain γ_f relative to their respective maximums.

displays very low average fracture strain when compared with these others. The difference therein lies in the associated heat treatments, with trials 2, 6, and 9 having low heat-treatment times of either 0 or 5 min, whereas trial 3 used the extended 20-min heat-treatment time. Trials 5 and 7 show poor ductility and were also treated for 20 min, leading to the assumption that extended heat-treatment times result in ductility loss. This is consistent with effects of the recrystallization induced in the PLA by heating, which results in a stronger, generally more brittle material.¹⁷

An additional inspection of the stress–strain response also reveals some detrimental behavior induced when utilizing a heat-treatment procedure on FDM PLA parts. As was noted in the Experimental section, although an increase in annealing time showed a high increase in strength, there was no discernable trend in the increases beyond the 10-min mark. The most notable feature is an increase in the variance of results, which is readily observable between the samples of each trial as shown in Fig. 7c, which compares all specimens that underwent a 20-min heat treatment. By contrast, those

with little to no heat treatment show less scatter in the height, shape, and length of the curves, as seen in Fig. 7a and b. The 5-min annealing trials show the least scattering of results, with all but one curve conforming to the same qualitative profile for each run, as visible in Fig. 7b. Overall, this indicates an increase in variance of material properties for parts heat treated for periods longer than 5 or 10 min, which is further supported by the results acquired in the heat-treatment time-variation experiment.

The microstructures pictured in Fig. 8 compare the internal structure of a 0.3-mm layer thickness and 60% infill component treated at 100°C for 20 min to an untreated sample. Based on these representative views, it can be inferred that the increase in heat-treatment time correlates to an increase in the inclusion of flaws within the PLA. Most notably, gas bubbles are formed within the heated sample of Fig. 8b, which create sites for crack initiation, which eventually propagates throughout the structure and leads to failure. It is conjectured that the random sizes and locations of these bubbles could be a significant contributor to the varied properties between samples. An inspec-

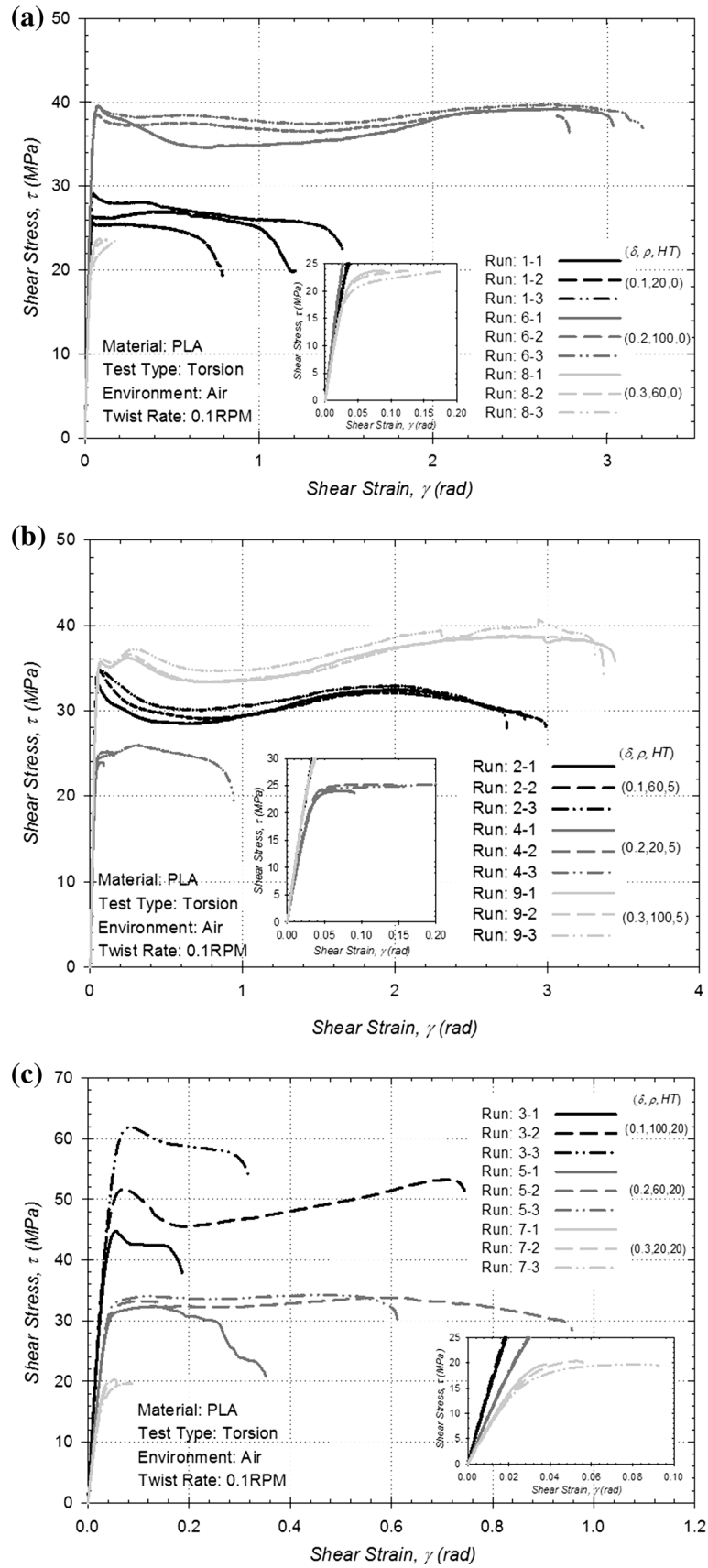


Fig. 7. Shear stress–strain response curves of all samples tested grouped by heat-treatment times of (a) 0 min, (b) 5 min, and (c) 20 min to emphasize the variance in material properties induced by extended heating times.

Table IV. ANOVA ranking table indicating influence of process parameters on specified material properties and preferred setting for each

Parameter ranking by influence on property			
Material property	1st	2nd	3rd
0.2% shear yield strength (τ_y)	Infill ³	Thickness ¹	Heat treatment ³
Ultimate shear strength (S_{us})	Infill ³	Thickness ¹	Heat treatment ³
Fracture strain (γ_f)	Infill ³	Heat treatment ^{1, 2}	Thickness ¹
Shear modulus (G)	Infill ³	Thickness ¹	Heat treatment ³
Proportional limit (τ_{pl})	Infill ³	Thickness ¹	Heat treatment ³

Within the table, 1 = low setting, 2 = middle setting, and 3 = high setting.

tion of Fig. 8b also reveals some shrinkage of the individual strands and shows that the outer perimeter of each strand has changed in color and opacity—a visual indicator of heating-induced recrystallization of the PLA.

ANOVA

A further examination of experimental mechanics results was conducted via regression analysis and ANOVA, which evaluates the variance between different groups to weigh the overall effects of each process parameter on performance. The regression analysis was run using the program Quantum XL (SigmaZone, Orlando, FL). Pareto plots of these results in Fig. 9 indicate the level of the effect on each material property. The values assigned to the parameters for each property on the Pareto plots have been normalized by the average of all of the parameters' scores for the property of interest so as to align them to a common scale. These have been catalogued in two distinct groupings: by material property and by processing parameter. The parameter-based grouping shows that infill unequivocally has the greatest impact on all resultant material properties. Contrastingly, heat treatment has only a slight effect on the metrics purely associated with strength when compared with those metrics that give an indication of ductility. The influence of layer thickness, although significant, rates lower than that of infill, and it has only a slight effect on the fracture strain. The groupings of thickness and heat treatment show an almost inverse effect for all but the shear modulus, which has an intermediate rating in both groupings. These associations are corroborated by the material property grouping, which shows the percentage contribution of each parameter on each property. The ultimate shear strength is heavily dependent on infill as compared with the other parameters; infill makes a 56% contribution, which is nearly twice that made by the thickness and four times as influential as the heat treatment. For the proportional limit and yield strength, the influence of the infill is

closely matched by the layer thickness with only a 7% difference in influence between the two parameters for both properties. Heat treatment rates at an average of 10% influence for these properties, indicating that elasticity is nearly wholly and equally dependent on both percentage infill and layer thickness. Conversely, the fracture strain, and consequently the ductility, is largely affected by the heat treatment, and the thickness has only a slight effect at 8% influence. The nearly equal reversal of the influence levels between the thickness and heat treatment for the elasticity and ductility metrics suggests a conflict between the parameter settings necessary to optimize for these characteristics. The shear modulus is the least disparately affected by the parameters, as it is a measure related to both strength and ductility.

To make a recommendation for the optimization of specific material properties, the Pareto plots and ANOVA results were aggregated to create an ANOVA ranking table⁹ (Table IV). The ANOVA ranking table summarizes the influence ranking of each parameter as well as the setting favored to optimize for the property of interest. Each process parameter is ranked from first to third in descending order of importance, and is marked with a value of 1 indicating the low setting, 2 the middle setting, and 3 the high setting as defined in Table II. The combination of 100% infill in combination with the low thickness setting of 0.1 mm is favored to achieve maximums for all material property values. However, whereas all of the strength metrics improved when using the high heat-treatment setting of 20 min, the fracture strain is highest when heat treatment is forgone or minimized. This means that strength and ductility, as can often be the case, result in conflicting settings when it comes to optimizing for either one.

OPTIMIZATION

Recommendations can be made for the optimization of mechanical properties based on the experimental mechanics results and their subsequent

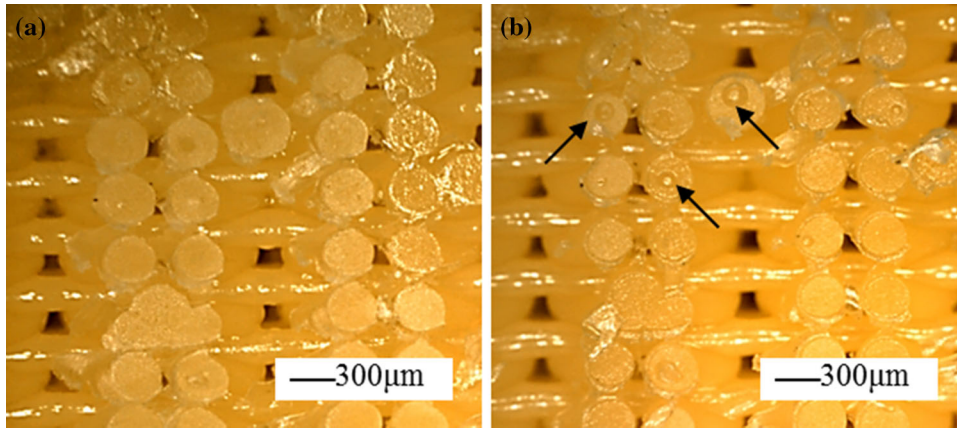


Fig. 8. Microstructure of a component in (a) as-printed condition (0 min HT) and (b) after 20 min of heat treatment. Arrows emphasize the random growth, placement, and size of inclusions caused by heating.

statistical analysis. As seen in Table IV, regardless of which mechanical property is being optimized, the layer thickness δ should always be set to the smallest thickness possible. The infill density ρ should always be maximized to maximize strength and resistance to failure as is shown both here and in the previous work,⁹ which focused on tensile and fracture experiments. Higher infill means more available material to resist deformation, regardless of the loading type. The heat treatment, however, is a conflicting parameter setting when optimizing for strength or ductility. Although an increase in heat-treatment time is associated with an increase in strength, especially for low infill parts, it is also associated with a decrease in ductility. To optimize solely for strength, the higher 20-min treatment time is recommended. Times beyond this point indicate no discernable differences in performance and an unfavorable increase in variance. For an emphasis on ductility, however, little to no heat treatment is recommended. It is recommended to favor a heat-treatment time of 5 min for general use, which results in a favorable balance of strength and ductility.

With the prediction model created by the regression analysis, it can be seen that the loss in strength with a decreased heat-treatment time is significantly smaller than the loss in ductility resulting from increasing heat-treatment time. For example, the prediction model using 0.1-mm layer height and 100% infill forecasts an 8% increase in S_{us} when increasing the heat-treatment time from 5 min to 20 min, but at a 67% reduction in γ_f . The recommendation to employ a short treatment time is further substantiated by earlier observations of Figs. 3, 7, and 8, which showed that an increase in heat-treatment time leads to greater variance in resulting material properties along with an increase in the internal flaws of the component microstructure. The prediction model further corroborates this finding, with the expected variance for S_{us} doubling

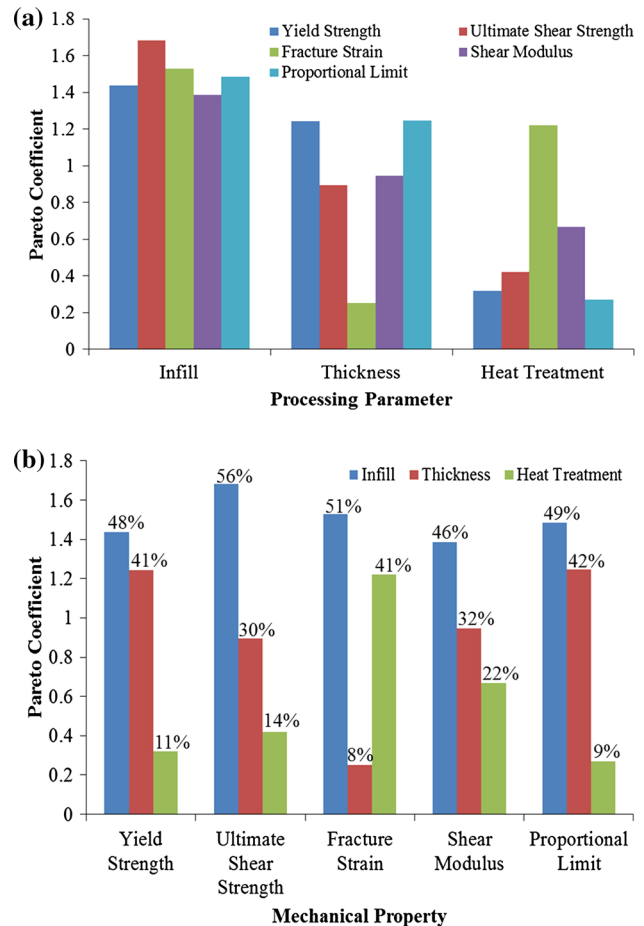


Fig. 9. Pareto plots depicting relative influence levels and percentage contributions of process parameters to resultant material properties organized by (a) process parameter and (b) material property.

when changing from no treatment to 20 min of heat treatment.

The highest calculated shear modulus value, which resulted from the average of the run 3 trials characterized by 0.1 mm layer thickness, 100% in-

fill, and 20 min heat-treatment time, was 1265 MPa, about 98% of the bulk value reported earlier of 1287 MPa. Using the von Mises yield criterion to equate the shear and tensile strength strengths as

$$S_{us} = 0.57S_{ut} \quad (4)$$

shows similar results. The average values of S_{us} achieved for the runs, which used 100% infill, runs 3, 6, and 9, were 53.35 MPa, 39.54 MPa, and 39.42 MPa, respectively. These values are analogous to the shear strength of 42.15 MPa calculated using the cited S_{ut} value of 73 MPa with the von Mises yield criterion. It can therefore be said that FDM components can closely match the behavior of those produced from bulk if the method suggested is used to properly optimize for the desired properties.

CONCLUSION

FDM PLA components were tested in torsion, and the effects of processing parameters including layer thickness, percent infill, and post-processing via heat treatment on the resultant shear properties were evaluated. A Taguchi L9 orthogonal array was defined and actualized with three repetitions for each experiment.

The effects of heat treatment were explored thoroughly as they relate to material properties and reliability. Although heat treatment can cause an increase in strength, especially in low-infill components such as those tested in the heat-treatment experiment trials, a large loss in ductility and an increase in the variance of resultant material properties accompanies the increase in strength. As such, low levels of heat treatment were suggested to improve strength while preserving ductility and reliability.

A previously used method for optimization of the material properties of FDM PLA components was validated and expanded upon. An in-depth analysis of the contributions of processing parameters on select mechanical properties was given. A method for compromising between conflicting properties was explored, which could extend these methods to other rapid prototyping technologies and materials to establish processing routines that balance conflicting resultant properties such as strength and ductility.

Guidelines were suggested for optimizing various properties of components in shear. It has been

shown that bulk PLA properties can be potentially achieved in FDM components using proper processing parameters and print orientation, though further research should be conducted for substantiation.

ACKNOWLEDGEMENTS

The participation of José Cotelo is made possible via the support of the Career Advancement Mentoring Program for Young Entrepreneur and Scholars (CAMP-YES), a National Science Foundation funded program at the University of Central Florida. Fabrication of test coupons was made possible due to the cooperation of the Center for Microgravity Research and Education at the University of Central Florida.

REFERENCES

1. M. Bijarimi, S. Ahmad, and R. Rasid, *Int. Conf. Agric. Chem. Environ. Sci.* 1, 115 (2012).
2. A.M. Clarinval and J. Halleux, *Biodegradable Polymers for Industrial Applications*, ed. R. Smith (Boca Raton: Taylor & Francis, 2005), pp. 3–31.
3. M. Jamshidian, E.A. Tehrani, M. Imran, M. Jacquot, and S. Desobry, *Comp. Rev. Food Sci.* 9, 552 (2010).
4. C.S. Lee, S.G. Kim, H.J. Kim, and S.H. Ahn, *J. Mater. Process. Tech.* 187–188, 627 (2007).
5. S.K. Panda, S. Padhee, A.K. Sood, and S.S. Mahapatra, *Intell. Inf. Manage.* 1, 89 (2009).
6. J.W. Zhang and A.H. Peng, *Adv. Mater. Res.* 538–541, 444 (2012).
7. G. Perego, G.D. Cella, and C. Bastioli, *J. Appl. Polym. Sci.* 59, 37 (1996).
8. M. Kowalczyk and E. Piorkowska, *J. Appl. Polym. Sci.* 124, 4579 (2012).
9. J. Torres, M. Cole, A. Owji, Z. DeMastry, and A.P. Gordon, *Rapid Prototyping J.* (in press).
10. A.K. Sood, R.K. Ohdar, and S.S. Mahapatra, *Mater. Des.* 31, 287 (2010).
11. J. Wootthikanokkhan, T. Cheachun, N. Sombatsompop, S. Thumsorn, N. Kaabbuathong, N. Wongta, J. Wong-On, S.I.N. Ayutthaya, and A. Kositchaiyong, *J. Appl. Polym. Sci.* 129, 215 (2013).
12. Y. Srithep, P. Nealey, and L.-S. Turng, *Polym. Eng. Sci.* 53, 580 (2013).
13. S.D. Park, M. Todo, K. Arakawa, and M. Koganemaru, *Polymer* 47, 1357 (2006).
14. A.M. Harris and E.C. Lee, *J. Appl. Polym. Sci.* 107, 2246 (2008).
15. J.H. Lin, H.Y. Chung, K.D. Wu, S.P. Wen, C.T. Lu, and C.W. Lou, *Adv. Mater. Res.* 627, 751 (2012).
16. A.P. Mathew, K. Oksman, and M. Sain, *J. Appl. Polym. Sci.* 97, 2014 (2005).
17. A. Galeski, *Prog. Polym. Sci.* 28, 1643 (2003).